IV Escola de Primavera de Transição e Turbulência
Universidade Federal do Rio Grande do Sul
Pontifícia Universidade Católica do Rio Grande do Sul
Porto Alegre, RS, 27 de setembro a 1º de outubro de 2004

LARGE-EDDY SIMULATION OF FLOWS IN TRANSITION TO TURBULENCE IN ANNULAR CHANNEL WITH HEAT TRANSFER, USING DYNAMIC SUB-GRID SCALE MODEL

Elie Luis Martínez Padilla
Federal University of Uberlândia
epadilla@mecanica.ufu.br

Aristeu da Silveira Neto
Federal University of Uberlândia
School of Mechanical Enginnering
Uberlândia, MG, Brazil 38400-902
aristeus@mecanica.ufu.br

Abstract. *In the present work three-dimensional numerical study of the transitional flow in natural convection in an horizontal annulus was performed using the Large-Eddy Simulation methodology with dynamical sub-grid scale model. The onset of the transition and turbulent regimes are pointed out. The characteristics of the unstable flow and the influence on heat transfer coefficient were analyzed. A comparative analyses involving tree kind of second filtering process, was also presented.*

Keywords. *Transition, large-eddy simulation, dynamic sub-grid scale model*

1. Introduction

The study of the natural convection between concentric cylinders has been the aim of several numerical and experimental investigations since the 30's, due to the enormous quantity of practical and technological applications. In the recent years, many numerical works have been done, some of them of three-dimensional approach.

One of the first works that studied the natural convection between concentric horizontal cylinders was due to Beckmann (1931), who used air, hydrogen, and carbon dioxide in order to analyze the type of fluid and the cylinders radii radio influence on the global heat transfer. Several later investigations, among them Voig & Krischer (1932), Kraussold (1934), and Grigull & Hauf (1966), have studied the effects on the local and global heat transfer due to the changes in the several parameters involved. The advances in the experimental techniques have allowed obtaining more information and details about the flow pattern, as can be seen in Bishop & Carley (1966) and Kuehn & Goldstein (1978). Among the few works that show and describes the flow destabilization in more details are Kuehn & Goldstein (1978) and McLeod & Bishop (1989). Kuehn & Goldstein (1978) have studied cylindrical concentric geometries filled with pressurized hydrogen over a wide range of Rayleigh number, corresponding to $2{,}2\text{x}10^2 \le Ra \le 7{,}7\text{x}10^7$ and radii radio of 2,6. The results have shown that the flow becomes, initially, unstable on the plume region (cavity's upper area) of about $Ra = 2\text{x}10^5$, changing to an fully turbulent condition as the Rayleigh number increases. At high Ra, they have reported the simultaneous coexistence of a highly turbulent zone and a stable laminar flow inside the cavity's lower part. McLeod e Bishop (1989) studied the problem using helium at cryogenic temperatures, changing the Rayleigh number of $8\text{x}10^6 \le Ra \le 2\text{x}10^9$, expansion number of $0{,}25 \le \beta\Delta T \le 1{,}0$, and diameter radio of $3{,}36 \le D_o / D_i \le 4{,}85$. As the results of their observations, they have graphically represented the dramatic changes when the Ra number is increased, and new flow structures in enclosure upper part have been found. It has been found, also, that an increment on the expansion number at a constant *Ra* number, developes a more turbulence intensity inside the enclosure. The referred graphic representations have revealed, at $Ra = 10^7$, an unstable thermal plume oscillating from right to left and vice-versa and, in the cavity's lower part, a stagnation region. The majority of the cited authors presented correlations to the heat transfer coefficient calculus. Itoh *et al*. (1970) presented, also, an interesting correlation based on a new definition for the characteristic length employed in the Rayleigh number evaluation.

The theoretical analysis about the convection between concentric cylinders has been, initially, performed by analytical solutions of series expansion and perturbation method and, afterwards, the boundary-layer theory was employed. After Crawford & Lemlich (1962), that used a Gauss-Seidel method, the numerical solutions have been shown a promising tool. Several techniques and methodologies have been used to solve the natural convection between horizontal concentric cylinders in laminar regime as well as the turbulent one. Some laminar flow references are Shibayama & Mashimo (1968), Powe et al. (1971), Kuehn & Goldstein (1976), Van de Sande & Hamer (1979), and Tsui & Templay (1983), noting that the later two works emphatized the transient behaviour. Studies on two-dimensional turbulent flow with $k-\varepsilon$ modeling are presented by Farouk & Güçeri (1982) and Char & Hsu (1998), the former considering vertical symmetry.

There are few three-dimensional approaches, as can be seen in laminar regime in Fusegi & Farouk (1986), Vafai & Ettefag (1991) & Vafai e Desai (1993). Desai e Vafai (1994) employed Van Driest mix length and $k-\varepsilon$ Standard to analyse the flow at $10^6 \le Ra \le 10^9$, several Prandtl number and radii ratio, and considering a closed cavity and symmetry in two directions, reducing the computational domain in ¾ of its original size. Information about the unstable behavior of the turbulent natural convection in periodic horizontal annuli is found in Fukuda *et al*. (1990) and Miki *et al*. (1993).

Fukuda *et al.* (1990) have employed the Direct Numerical Simulation (DNS) to study problems for Rayleigh up to $5x10^5$, Prandtl number of 0,71, radii ratio of 2,0, and aspect ratio of 2,8. The results made possible to predict the transition flow oscillations, as well as characteristic heated plume movement, and have shown that they diverge from the experimental data as the turbulence increases. On the other hand, Miki et al. (1993) have used the Large Eddy Simulation methodology with Smagorinsky sub-grid scale model, considering several radii ratio, aspect ratio, Smagorinsky constant and Prandtl number, and Rayleigh numbers of $2{,}5x10^6 \leq Ra \leq 1{,}18x10^9$. The effects of these parameters on the turbulent characteristics were evaluated.

In this work, numerical studies of the transition phenomena inside horizontal annuli in natural convection are presented, having periodicity condition in axial plane, and Large-Eddy Simulation methodology with dynamic sub-grid scale modeling.

2. Numerical Method

An incompressible and newtonian flow (air), having constant physical proprieties are considered. The buoyancy term, related to the fluid density change, caused mainly for the fluid thermal expansion, is modeled by the Boussinesq approximation. The flow having cinematic viscosity ν and density ρ, are inside an annuli formed by two horizontal concentric cylinders of radii R_i and R_o, corresponding to inner and outer cylinder, respectively. As observed in Fig. 1, the cylinders are isothermic surfaces at T_i and T_o, where the inner cylinder temperature is higher than the outer one. The space between cylinders is labeled $L = R_o - R_i$ and the axial length L_{ax}. The geometric characteristics are defined by the parameters: radii ratio $\eta = R_o / R_i$ and aspect ratio $\Gamma = L_{ax} / L$.

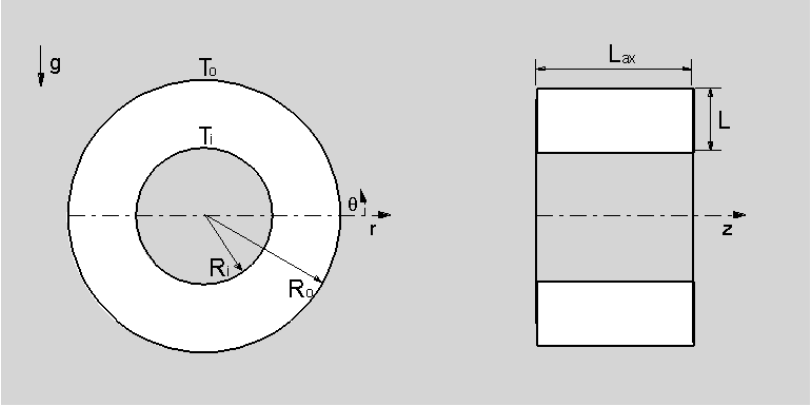

Figure 1. Cavity between concentric cylinders.

The problem presented in this work is governed by the Navier-Stokes equations and the energy conservation, in which the filtering process are applied, allowing separating the sub-grid field from the large scales. This filtering process gives rise to the generalized sub-grid Reynolds stress tensor, defined as $\tau_{ij} = -(\overline{u_i u_j} - \overline{u}_i \overline{u}_j)$ and to the generalized sub-grid turbulent flux, defined as $q_{t_j} = -(\overline{u_j T} - \overline{u}_j \overline{T})$, as described by Silveira-Neto et al. (2002).This tensor and this turbulent flow are modeled using the Boussinesq hypothesis.

$$\tau_{ij} = -\nu_t 2\overline{S}_{ij} + \frac{2}{3} k \delta_{ij}, \tag{1}$$

$$q_{t_j} = -\alpha_t \frac{\partial \overline{T}}{\partial x_j}, \tag{2}$$

where ν_t is the turbulent viscosity, $\overline{S}_{ij} = 0{,}5(\partial \overline{u}_i / \partial x_j + \partial \overline{u}_j / \partial x_i)$ is filtered field strain rate, k is the kinetic turbulent energy, δ_{ij} is the Dirac's δ-function, and α_t is the turbulent thermal diffusivity. The Eqs. (1) and (2) are added to the governing equations leading, finally, to:

$$\frac{\partial \overline{u}_j}{\partial x_j} = 0, \tag{3}$$

$$\frac{\partial \overline{u}_i}{\partial t} + \frac{\partial (\overline{u}_i \overline{u}_j)}{\partial x_j} = -\frac{1}{\rho_0}\frac{\partial \overline{p}}{\partial x_j} - \beta \Delta \overline{T} g_i + \frac{\partial}{\partial x_j}\left[(\nu + \nu_t)\left(\frac{\partial \overline{u}_i}{\partial x_j} + \frac{\partial \overline{u}_j}{\partial x_i} \right) \right], \tag{4}$$

$$\frac{\partial \overline{T}}{\partial t} + \frac{\partial (\overline{u}_j \overline{T})}{\partial x_j} = \frac{\partial}{\partial x_j}\left[(\alpha + \alpha_t)\frac{\partial \overline{T}}{\partial x_j} \right], \tag{5}$$

where ρ_o represents the density at bulk temperature, β is the thermal expansion coefficient and, g_i is the gravity acceleration. The dynamic sub-grid scale model (Germano et al., 1991) allows the turbulent viscosity evaluation according to the expression presented by Lilly (1991):

$$\nu_t = C(\vec{x},t)(\overline{\Delta})^2 \mid \overline{S} \mid, \tag{6}$$

$$C(\vec{x},t) = -\frac{1}{2}\frac{L_{ij} M_{ij}}{M_{ij} M_{ij}}. \tag{7}$$

According to the Eq. (6), the turbulent viscosity is directly related to the dynamic coefficient $C(\vec{x},t)$, filter characteristic length $\overline{\Delta}$, and the strain tensor modulus $|\overline{S}|$. The dynamic coefficient depends on the global Leonard tensor $L_{ij} = \overline{u}_i \overline{u}_j - \widehat{\overline{u}_i \overline{u}_j}$ and on the tensor $M_{ij} = (\hat{\overline{\Delta}})^2 \mid \hat{\overline{S}} \mid \hat{\overline{S}}_{ij} - \widehat{(\overline{\Delta})^2 \mid \overline{S} \mid \overline{S}_{ij}}$, where the operator [^] indicates the second filtering process, as recommended in Padilla & Siveira-Neto (2003). The turbulent thermal diffusivity is evaluated using the turbulent Prandtl number, as done by Silveira-Neto et al. (1993).

The filtered equations (3-5) in cylindrical coordinates are non-dimensionalized by the inner and outer cylinders temperatures, the spacing between cylinders, the molecular viscosity, and the density. The boundary condition along the radial axis becomes:

$$u,\ v,\ w\ (R_i, \theta, z, t) = 0, \qquad T(R_i, \theta, z, t) = 1,$$

$$u,\ v,\ w\ (R_o, \theta, z, t) = 0, \qquad T(R_o, \theta, z, t) = 0.$$

Along the angular and axial directions, the periodicity condition is considered.

In order to perform the equations discretization, the finite volume method was employed in a staggered grid, having second order schemes in space and time (Piomelli, 2000 and Ferzinger & Peric, 1999): central differencing scheme and Adams-Bashforth, respectively. The pressure-velocity coupling method was the fractional time (Kim e Moin, 1985), where the steps named predictor and corrector are used. The pressure correction field is evaluated by solving the Poisson equation using SIP (Strongly Implicit Procedure) method, as proposed by Stone (1968).

The time step is evaluated following the CFL (Courant-Friedix e Lewi) stability criteria. Moreover, non-uniform meshes are employed along the radial direction, concentrated near walls (5% variation), and uniform along the remaining axes.

3. Results

The numerical analysis of the natural convection at low and moderate Rayleigh number, which represents stable flows, were presented in previous Works: Padilla (2004) and Padilla et al. (2004). In the present work, the flow pattern and its influence on the local and average heat transfer process are compared qualitatively and quantitatively against the experimental data from Kuehn e Goldstein (1976). Fig. 2 shows the local flow proprieties, for Ra=4.7x10^4, and geometric configuration of radii ratio of η=2.6 and aspect ratio of Γ=1, considering a mesh of 20x80x2 along the radial, angular, and axial axis, respectively. No sub-grid turbulence modeling was employed.

In the Figure 2(a), one has the temperature distribution along the radial direction for three values of θ=0°, 90° and 270° and, in the Fig. 2(b) the local Nusselt number distribution in the inner Nu_i and outer Nu_o walls, evaluated according to the definitions:

$$Nu_i = R_i \ln\left[\frac{R_o}{R_i}\right]\frac{\partial \overline{T}}{\partial r}\Big|_{r=R_i}, \qquad Nu_o = R_o \ln\left[\frac{R_o}{R_i}\right]\frac{\partial \overline{T}}{\partial r}\Big|_{r=R_o}. \tag{8}$$

Comparison com others authors indicates a good agreement to the experimental data, showing that the numerical code reproduces, accurately, flows with heat transfer inside horizontal concentric cylinders.

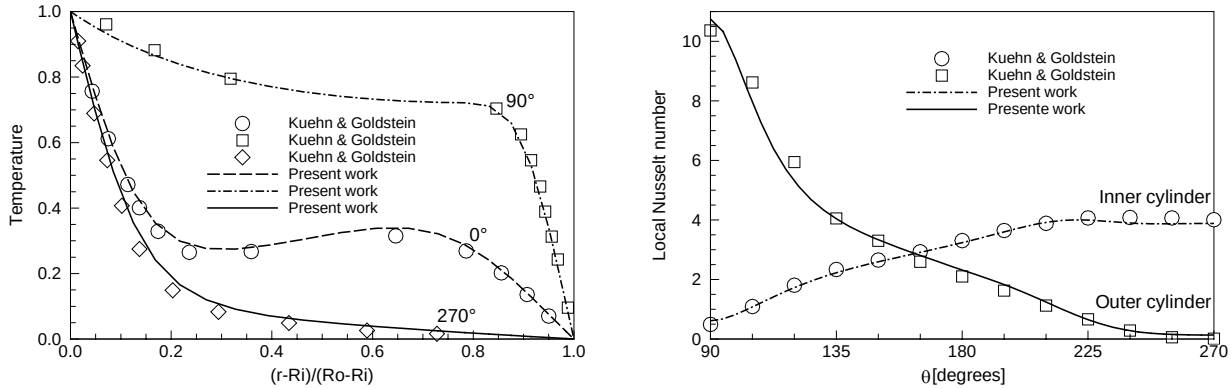

Figure 2. Comparison with experimental dates at Ra=4.7x10^4, η=2.6, Γ=1; (a) temperature distribution, (b) local Nusselt number.

3.1. Discrete Test Filters

An important question related to the use of dynamic sub-grid scale models is the application of the test filter, because the second filtering process would give information about the resolved scales to model the energy transfer between the two part of the energy spectrum. In this context, three discrete filters are suggested, denominated FA, FT and FP, respectively:

$$\hat{f}_{ijk} = \frac{1}{7}\left(\bar{f}_{i-1,j,k} + \bar{f}_{i+1,j,k} + \bar{f}_{i,j,k} + \bar{f}_{i,j-1,k} + \bar{f}_{i,j+1,k} + \bar{f}_{i,j,k-1} + \bar{f}_{i,j,k+1}\right), \tag{8}$$

$$\hat{f}_{ijk} = \frac{1}{8}\left(\bar{f}_{i-1,j,k} + \bar{f}_{i+1,j,k} + 2\,\bar{f}_{i,j,k} + \bar{f}_{i,j-1,k} + \bar{f}_{i,j+1,k} + \bar{f}_{i,j,k-1} + \bar{f}_{i,j,k+1}\right), \tag{9}$$

$$\hat{f}_{ijk} = (1-pp)\,\bar{f}_{MP} + (pp)\,\bar{f}_{ijk}, \tag{10}$$

where pp is the weight factor attributed to $\bar{f}_{ijk}$ and $\bar{f}_{MP}$ corresponds to the weighted average in function to the distance d between the adjacent volumes centers.

$$\bar{f}_{MP} = \frac{\bar{f}_{i-1,j,k}/d_{i-1} + \bar{f}_{i+1,j,k}/d_{i+1} + \bar{f}_{i,j-1,k}/d_{j-1} + \bar{f}_{i,j+1,k}/d_{j+1} + \bar{f}_{i,j,k-1}/d_{k-1} + \bar{f}_{i,j,k+1}/d_{k+1}}{1/d_{i-1} + 1/d_{i+1} + 1/d_{j-1} + 1/d_{j+1} + 1/d_{k-1} + 1/d_{k+1}} \tag{11}$$

Several simulation were performed to evaluate the influence of the test filters FA, FT e FP*pp*, with the weight factor pp=2 and 5, on the transition flow at Rayleigh number of Ra=1.7x10^5 and geometric parameters η=2 and Γ=2.8. The mesh considered in this analysis was the 12x60x20 cells. It is a stable flow characterized by the presence of three-dimensional oscillations, which allows evaluating the sub-grid scale model properly with different test filters. This case was, also, simulated without sub-grid modeling.

The time behavior of the radial and angular velocity components using several filters, as well as with or without sub-grid scale turbulence model, is presented in Fig. 3. The numerical probes signals were monitored at r=1.5, θ=90° and z=1.4 position. One observes different behavior in the frequency and amplitude for both velocity components, with the presence of great fluctuations for filters FT and FP05 cases. The differences observed in the average angular velocity with the FA filter, where that fluctuations appear, are enormous. Clear differences were observed, also, in the temporal behavior of the axial velocity component. Indeed, the flow dynamics change from each filter used.

It is well-known that the non-use of a sub-grid turbulence models in unstable flows implies in a underestimation of this kind of flow oscillations. However, the oscillations don't lead the simulations to diverge, which tend to consider the described dynamic behavior as valid. Coincidently, the FP02 filter behavior follows the no model case, though with smaller amplitudes.

In the Figure 4, one has the turbulent viscosity radial distribution and average temperature (timely) in 90° and z=1.4. The turbulent viscosity profile (Fig. 4a) describes an important characteristic of the dynamic model, observed near the cylinders walls, in which the turbulent viscosity tends to zero. The distribution with FP05 and FP02 filters shows a more coherent behavior. In the Fig. 4(b), the temperature profile, corresponding to the plume region, are compared against to the experimental data of Fukuda et al. (1990). Again, the filters FP05 and FP02 present a good behaviour, when compared against experimental data.

According to the results presented and a complete analysis done in Padilla & Silveira-Neto (2003) and Padilla (2004), where the qualitative characteristics are highlighted, the FP02 was considered the more suitable filter in order to perform the second filtering process.

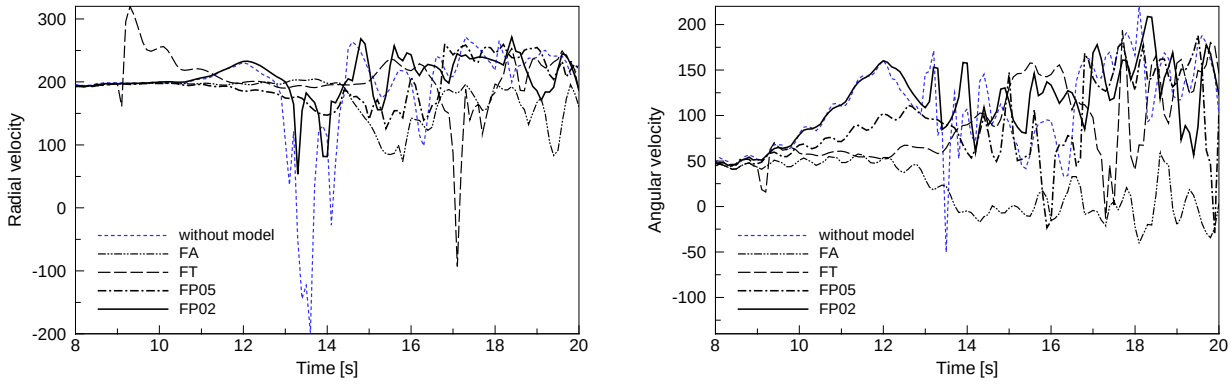

Figure 3. Influence of the several test filters over velocity fluctuations; (a) radial velocity (b) angular velocity.

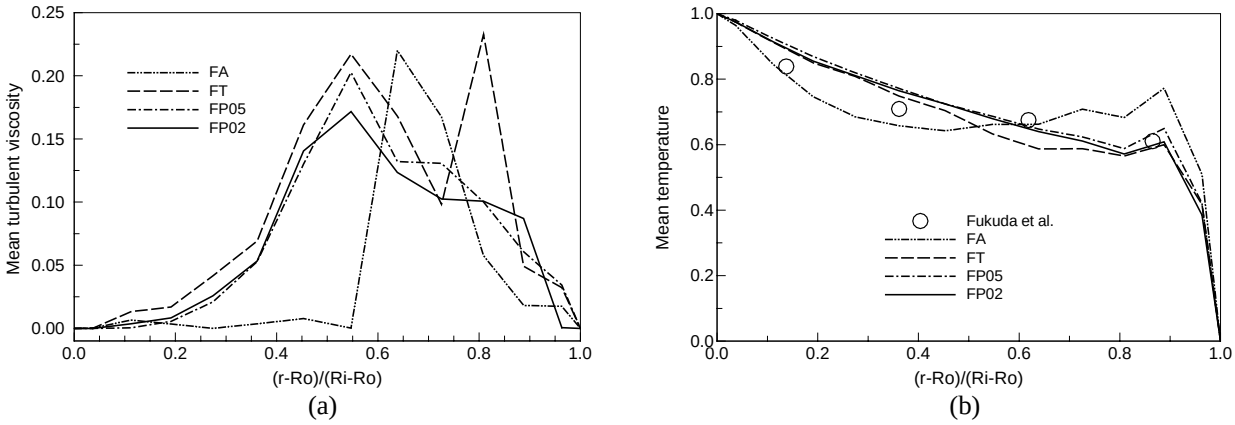

Figure 4. Influence of the several test filters over average-time proprieties; (a) turbulent viscosity, (b) temperature.

3.2. Transitional Flows

A study corresponding to the stable flows in horizontal annuli was done over a range of Rayleigh $4.6\text{x}10^4 \leq Ra \leq 7.5\text{x}10^5$, and geometric configuration of radii ratio of η=2 and aspect radio of Γ=2.8. Moreover, was employed a mesh having 16x72x24 cells along the radial, angular and axial directions, respectively. The computational costs is higher as the *Ra* increases, for example, in order to simulate only one second at $Ra=1.5\text{x}10^5$ is necessary 4.9 h in a 2.8 GHz Pentium IV.

According to Bishop et al. (1968), the instability onset appears at cavities upper part, becoming an oscillating behavior, where the oscillations increase as the *Ra* increases. It was possible to register, precisely, theses characteristics by a numerical probe located at r=1.5, θ =90° e z=1.4. Small periodic oscillations in the velocity and temperature field were observed at $Ra=4.7\text{x}10^4$. For higher *Ra* values these oscillations increases and changes drastically, as can be seen in Fig. 5. In this figure, the radial velocity component is depicted for four different *Ra* numbers. The fluctuations for $Ra=5.0\text{x}10^4$ are small and periodic, that oscillates at a fundamental frequency of 0.75 Hz. As the Rayleigh number increases, the oscillations lose its periodic behavior, augmenting its amplitude and frequency. From $Ra=1.5\text{x}10^5$ the oscillations start representing a certain irregular pattern, which at $Ra=7.5\text{x}10^7$ they present a complete irregular pattern and high amplitude, with the presence of a wide range of important frequencies, characterizing fully turbulent flow.

The effect of the dynamic instability on the temperature field manifest, initially, in the plume structure and after, in the other regions, as can be seen in the Fig. 6. In Figs. 6 and 7, instantaneous isothermal surfaces are depicted for three different Rayleigh numbers. The blue and yellow isosurfaces represents the non-dimensional temperatures of 0.65 and 0.25, respectively. One observe, in Fig. 6, that as the *Ra* is increased, the instabilities multiplies and intensifies, where the more affected region corresponds to the upper part of the cavity. In the flow corresponding to $Ra=1{,}0\text{x}10^5$ (Fig. 6a), the thermal plume oscillates axially, with small amplitudes and, also, small movements along the θ direction. For Rayleigh number $Ra=1.5\text{x}10^5$ (Fig. 6b), the oscillation represents high amplitudes and intense three-

dimensionalization, where the blue isosurfaces oscillations are notorious, mainly around 0° and 180°. For Ra =5.8x10^5 (Fig. 6c) one observes an irregular pattern with hot mass loosing in both sides, showing turbulent behaviour. The oscillations around 0° and 180° are very intense, noting that the cavity lower part is unstable, but less intense.

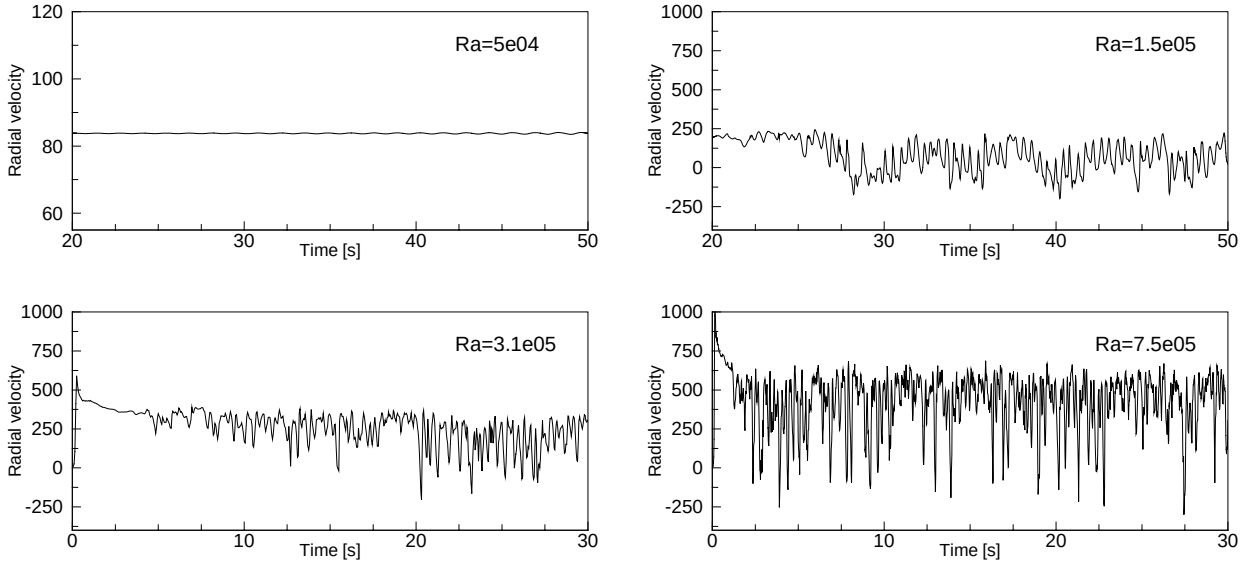

Figure 5. Radial velocity fluctuations at Ra =5x10^4, 1.5x10^5, 3.1x10^5, 7.5x10^5.

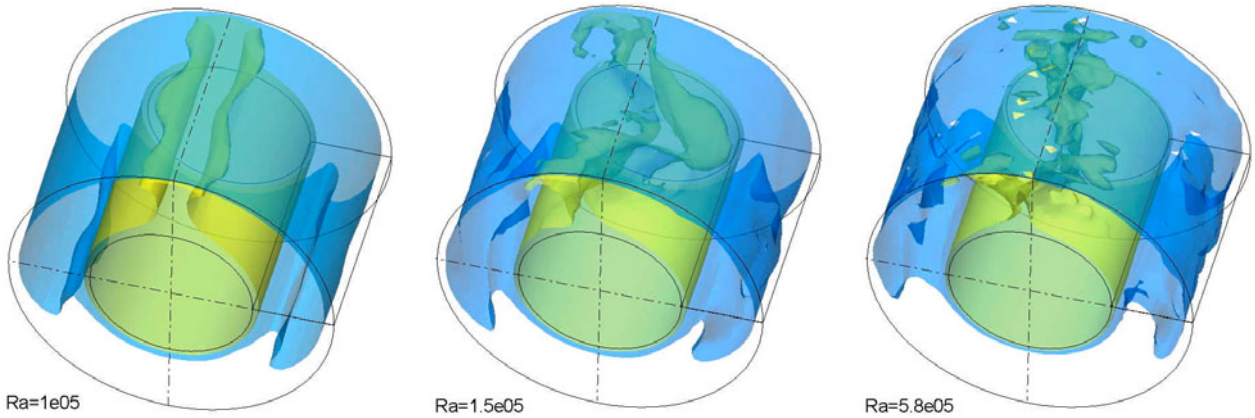

Figure 6. Instantaneous temperature isosurface, 25: blue and 0.65: yellow; (a) Ra =1x10^5, (b) Ra =1.5x10^5, (c) Ra =5.8x10^5.

In Figure 7, one depicts the flow time development at Ra =1,5x10^5 in three periods: 49, 49.5 and 50 s. The transitional flow presents oscillation in three dimensions. The plume oscillates periodically with high amplitude, moving from right (Fig. 7a) to left (Fig. 7b), and vice-versa, as experimentally demonstrated by Bishop et al. (1968), and Kuehn & Goldstein (1978).

The evaluation of average flow proprieties has allowed confirming the results coherence, where the radial and axial velocity components distribution presents a profile similar to the stable flows at moderate *Ra*, but without symmetry, referring to the vertical axial plane. The axial velocity component presents a magnitude lower than its other counterparts, indicating clearly the presence of recirculating flows.

The turbulent viscosity average behavior along the radial direction in θ=0°, 90°, 180° and 270° and z =1.4, for cases at Ra =1.5x10^5 and 5.8x10^5, are shown in the Figure 8. One can see its adequate behavior near the cylinders walls, and its nullification in parietal regions. The turbulent viscosity presents higher values as the Ra increases, demonstrating that the sub-grid scale model plays a role of increasing importance. The profile in 90° indicates that, at the upper cavity region, the instabilities has a higher intensity level, where the turbulent viscosity is 0.1 to 0.45 times the molecular viscosity at Ra =1.5x10^5 and 5.8x10^5, respectively.

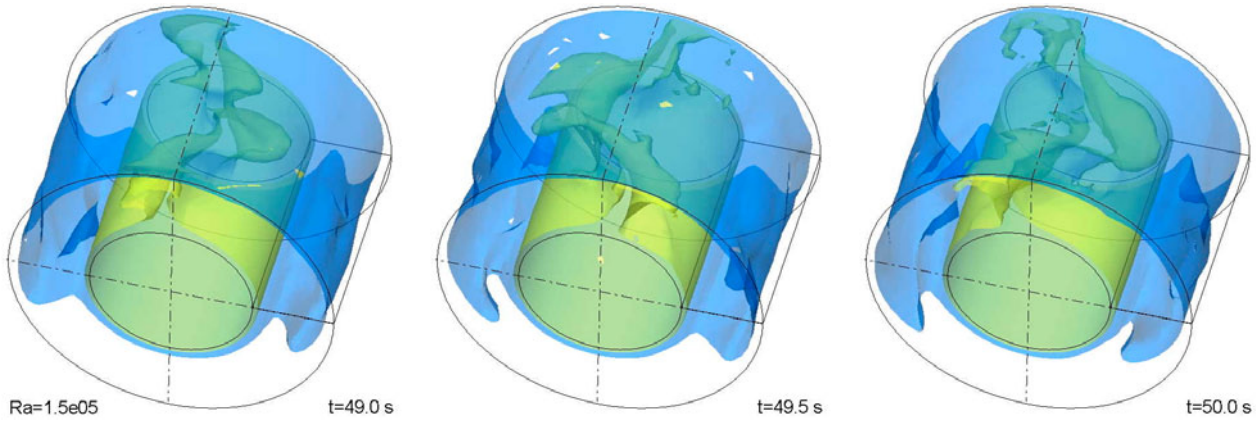

(a) (b) (c)

Figure 7. Temporal evolution of temperature isosurface for Ra =1,5x10^5; (a) 49 s, (b) 49.5 s, (c) 50 s.

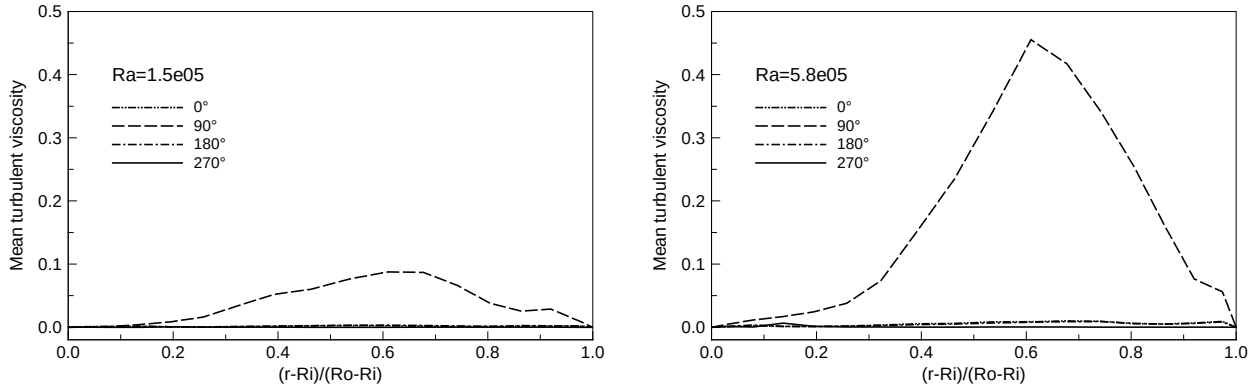

(a) (b)

Figure 8. Average-time turbulent viscosity at four values of θ; (a) Ra =1.5x10^5, (b) Ra =5.8x10^5.

The energy spectrum related to the radial velocity component fluctuation, at Ra =1.5x10^5 and 7.5x10^5, are presented in Figure 9. A line having the -5/3 inclination has been drawn, according to the Kolmogorov's law, which corresponds to spectrum inertial zone inclination at fully developed turbulence. One observe, also, that he flow energy increases as the *Ra* becomes higher. The spectrum at Ra =1.5x10^5 has inclination higher than -5/3, demonstrating an energy concentration in the large scales. On the other hand, increasing the Rayleigh number up to Ra =7.5x10^5, the energy is better distributed, "smoothing" the spectrum inclination to –5/3.

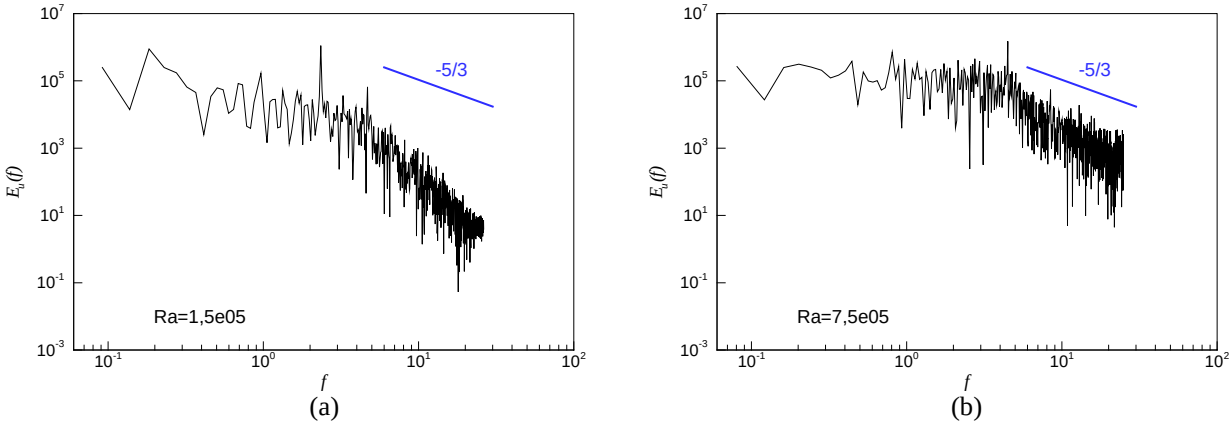

(a) (b)

Figure 9. Energy spectra of the radial velocity fluctuation at; (a) Ra =1.5x10^5, (b) Ra =7.5x10^5

The formation of structures inside the flow is a characteristic of unstable flows, that changes its topology as the Rayleigh number increases, and an example can be seen in Figure 10. In this figure, vorticities isosurfaces are depicted for ω_θ = 200 (grey) e –200 (green). At Ra =1.5x10^5, is evident the counter-rotating structures disposed in Λ shape at

cavity upper part, which orientation changes, following the plume oscillatory movement. For higher Rayleigh numbers, a disorganization process can be seen, as a result of the frequency multiplication.

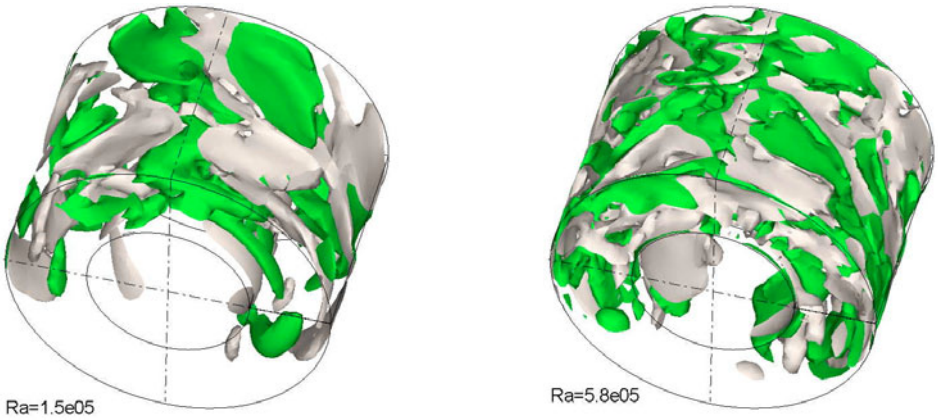

(a) (b)

Figure 10. Instantaneous vorticity isosurface, 200: grey and -200: green; (a) Ra =1.5x10^5, (b) Ra =5.8x10^5.

Fluctuations on the local and average Nusselt number, related to the inner and outer cylinders surfaces, are a consequence of the unstable dynamic behavior typical of transitioning to turbulence flows, which leads to a more efficient heat transfer process where. The average local Nusselt number also increases.

The global average Nusselt number distribution, as a function of the Rayleigh number is depicted in the Fig. 11. The results in the global average Nusselt number $\{Nu\}$ evaluation, that compounds the inner (Nu_i) and outer (Nu_o) space and time average, are compared against the Itoh et al. (1970) correlation, that used the composed characteristic length $r_m = \ln(R_i/R_o)\sqrt{R_i R_o}$ to evaluate the modified Grashof number. Experimental data leads to the expression $\{Nu\} = 0{,}18 Gr_m^{1/4}$. One can see that the agreement with the Itoh et al. (1970) correlation is very good for the entire transition to turbulence range. When comparing to Fukuda et al. (1990) numeric results, which predicts an higher turbulence intensity, the present work has better results than the former work.

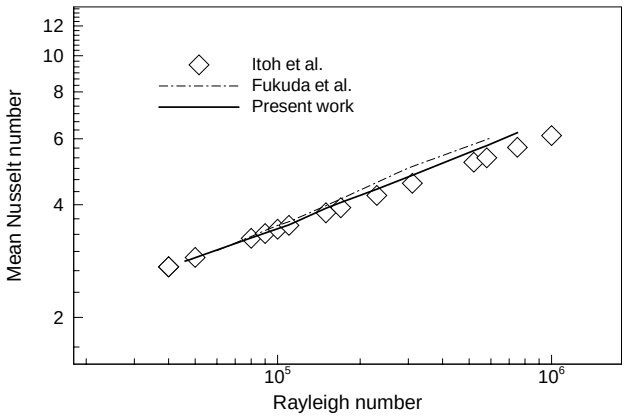

Figure 11. Mean Nusselt number as a function of Rayleigh number.

5. Conclusion

Numerical simulations of natural convection flows in transition to turbulence regime were successful performed employing Large-Eddy Simulation technique with dynamic sub-grid scale model. The results have evidenced the onset of the first instabilities that increases its intensity as the Rayleigh number increases, becoming fully irregular when the turbulent regime is reached. Moreover, it was possible to capture the flow dynamic characteristics, as well as the plume transition. A new test filter, suitable for non-uniform meshes in cylindrical coordinates, is proposed. Results compare very well with experimental and numerical results from others authors

Acknowledgement: The autors would like to tank Conselho Nacional de Desenvolvimento Científico e Tecnológico (CNPq) for the financial support.

5. References

Beckmann, W., 1931, "Die Wärmeübertragung in Zylindrischen Gasschichten bei Natürlicher Konvektion", Forschung auf dem Gebiete des Ingenieurwesens, Bd. 2, Heft 5, pp. 165-178.

Bishop, E. H. and Carley, C. T., 1966, "Photographic Studies of Natural Convection Between Concentric Cylinders", Proceedings of the 1966 Heat Transfer Fluid Mechanics Institute, pp. 63-78.

Bishop, E. H. and Carley, C. T., 1968, "Natural Convective Oscillatory Flow in Cylindrical Annuli", Int. J. Heat and Mass Transfer, vol. 11, pp. 1741-1752.

Char, M-I. and Hsu, Y.-H, 1998, "Numerical Prediction of Turbulent Mixed Convection in a Concentric Horizontal Rotating Annulus with Low-Re Two-Equation Models. Int. J. Heat Mass Transfer, vol. 41(12), pp. 1633-1643.

Crawford, L. and Lemlich, R., 1962, "Natural Convection in Horizontal Concentric Cylindrical Annuli", I. E. C. Fund., 1, pp. 260-264.

Desai, C. P., and Vafai, K., 1994, "An Investigation and Comparative Analysis of Two-and Tree-dimensional Turbulent natural convection in a Horizontal Annulus", I. J. Heat Mass Transfer, vol. 37(16), pp. 2475-2504.

Farouk, B. and Güceri, S. I., 1982, "Natural Convection From a Horizontal Cylinder-Laminar Regime", J. Heat Transfer, 103, pp. 522-527.

Ferzinger, J. H., Peric, M., 1999, "Computational Methods for Fluid Dynamics", 2nd. rev. ed. Springer, New York.

Fukuda, K., Miki, Y., and Hasegawa, S., 1990, "Analytical and Experimental Study on Turbulent Natural Convection in a Horizontal Annulus", Int. J. Heat Mass Transfer, vol. 33(4), pp. 629-639.

Fusegi, T. and Farouk, B., 1986, "A Tree-dimensional Study of Natural Convection in the Annulus Between, Horizontal Concentric Cylinder", Proc. 8th Int. Heat Transfer Conf., vol. 4, pp. 1575-1580.

Germano, M., Piomelli, U., Moin, P. and Cabot, W. H., 1991, "A Dynamic Sub-Grid-Scale Eddy Viscosity Model", Phys. Fluids A 3 (7) July, pp. 1760-1765.

Grigull, U. and Hauf, W., 1966, "Natural Convection in Horizontal Cylindrical Annuli", Third Int. Heat Transfer Conf., pp. 182-195.

Itoh, M., Fujita, T., Nishiwaki, N. and Hirata, M., 1970, "A New Method of Correlating Heat-Transfer Coefficients for Natural Convection in Horizontal Cylindrical Annuli", Int. J. Heat Mass Transfer, vol. 13, pp. 1364-1369.

Kim, J. and Moin, P., 1985, "Application of a Fractional Step Method to Incompressible Navier-Stokes Equations", J. Comp. Phys., 59, pp. 308-323.

Kraussold, H., 1934, "Wärmeabgabe von Zylindrischen Flüssigkeitschichten bei Natürlicher Konvektion", Forschung auf dem Gebiete des Ingenieurwesens. Bd. 5, Heft 4, pp. 186-191.

Kuehn, T. H. and Goldstein, R. J., 1976, "Correlating Equations for Natural Convection Heat Transfer Between Circular Cylinders", Int. J. Heat and Mass Transfer, vol. 19, pp. 1127-1134.

Kuehn T. H. and Goldstein, R. J., 1978, "An Experimental Study of Natural Convection Heat Transfer in Concentric and Eccentric Horizontal Cylindrical Annuli", ASME J. of Heat Transfer, vol. 100, pp. 635-640.

Lilly, D. K., 1991, "A Proposed Modification of the Germano Subgrid-Scale Closure Method", Phys. Fluids A 4 (3). March, American Institute of Physics, pp. 633-635.

McLeod, A. E. and Bishop, E. H., 1989, "Turbulent Natural Convection of Gases in Horizontal Cylindrical Annuli at Cryogenic Temperatures", Int. J. Heat Mass Transfer, vol. 32(10), pp. 1967-1978.

Miki, Y., Fukuda, K. and Taniguchi, N., 1993, "Large Eddy Simulation of Turbulent Natural Convection in Concentric Horizontal Annuli", Int. J. Heat and Fluid Flow, vol. 14(3), pp. 210-216.

Padilla, E. L. M., e Silveira Neto, A., 2003, "Influência de Diferentes Tipos de Filtros para Modelagem Dinâmica em Simulação de Grandes Escalas", XXIV Iberiam Latin-American Congress on Computational Methods in Engineering, Ouro Preto-MG, Brasil, pp. CIL189-32.

Padilla, E. L. M., 2004, "Large-Eddy Simulation of Transition to Turbulence in Rotating Sistem with Heat Transfer", Doctor Thesis, Universidade Federal de Uberlândia, MG.

Padilla, E. L. M., Campregher, R. e Silveira Neto, A., 2004, "Numerical Analysis of the Laminar Natural Convection in Concentric Horizontal Cylindrical Annuli", VI Simpósio Mineiro de Mecânica Computacional", Itajubá-MG, Brasil, pp. MF-02.

Piomelli, U., Scotti, A. and Balaras, E., 2000, "Large-Eddy Simulations of Turbulent Flows, from Desktop to Supercomputer", Fourth International Conference on Vector and Parallel Processing, J. M. L. M. Palma, J. Dongarra and V. Hernàndez, Springer: Berlin, pp. 551-577.

Powe, R. E., Carley, C. T. and Carruth, S. L., 1971, "A Numerical Solution for Natural Convection in Cylindrical Annuli", J. Heat Transfer, 92(12), pp. 210-220.

Shibayama, S. and Mashimo, Y., 1968, "Natural Convection Heat Transfer in Horizontal Concentric Cylindrical Annuli", Papers J. S. M. E. Nat. Symp., n. 169. pp.7-20.

Silveira-Neto, A., Mansur, S. S. and Silvestrini, J. H., 2002, "Equações da turbulência: Média versus Filtragem", III Escola de Primavera de Transição e Turbulência, Anais, pp. 1-7.

Silveira-Neto, A., Grand, D., Metais, O. and Lesieur, M., 1993, "A Numerical Investigation of the Coherent Structures of Turbulence Behind a Backward-Facing Step", Int. Journal of Fluids Mechanics, vol. 256, pp. 1-25.

Stone, H. L., 1968, "Iterative Solution of Implicit Approximations of Multidimensional Partial Differential Equations", SIAMJ Numer. Anal., vol. 5, pp. 530-558.

Tsui, Y. T. and Temblay, B., 1983, “On Transient Natural Convection Heat Transfer in the Annulus Between Concentric, Horizontal Cylinders with Isothermal Surfaces”, Int. J. Heat Mass Transfer, vol. 27, pp.103-111.

Vafai, K., and Ettefagh, J., 1991, “An Investigation of Transient Tree-dimensional Buoyancy-driven Flow and Heat Transfer in a Closed Horizontal Annulus”, Int. J. Heat Mass Transfer, vol. 34(10), pp. 2555-2570.

Vafai, K., and Desai, C. P., 1993, “Comparative Analysis of the Finite-element and Finite-difference Methods for Simulation of Buoyancy-induced Flow and Heat Transfer in Closed and Open Ended Annular Cavities”, Numerical Heat Transfer, vol. 23(A), pp. 35-59.

Van de Sande, E. and Hamer, B. J. G., 1979, “Steady and Natural Convection in Enclosures Between Horizontal Circular Cylinders (Constant Heat Flux)”, Int. J. Heat Mass Transfer, vol. 22, pp. 361-370.

Voig, H. and Krischer, O., 1932, “Die Wärmeübertragung in Zylindrischen Luftschichten bei Natürlicher Konvektion”, Forsh. Grn. D. Ingenieurwesen, 3(6), pp. 303-306.